Inorganic Chemistry

ARTICLE

pubs.acs.org/IC

Reinvestigation of the OP4-(Li/Na)CoO_2-Layered System and First Evidence of the (Li/Na/Na)CoO_2 Phase with OPP9 Oxygen Stacking

R. Berthelot,[†,‡] M. Pollet,[*,†] D. Carlier,[†,§] and C. Delmas[†]

[†]CNRS, Université de Bordeaux, ICMCB, 87 avenue du Dr. A. Schweitzer, 33608-F Pessac, France

[‡]CEA-Grenoble, DRT-LITEN, 17 rue des Martyrs, 38054 Grenoble, France

[§]CNRS, ENSCBP, ICMCB, 87 avenue du Dr. Schweitzer, 33608-F Pessac, France

ABSTRACT: The composition and synthesis conditions of the (Li/Na)CoO_2 phase with an ordered 1:1 Li/Na stacking alternating with CoO_2 slabs were determined from a careful study of the P2-$Na_{\sim 0.7}CoO_2$−O3-$LiCoO_2$ system. An in situ X-ray diffraction (XRD) thermal study emphasizes the metastable character of this phase that can be stabilized only by very fast quenching. Its composition, $(Li_{0.42}Na_{0.37})CoO_2$, is significantly different from the ideally expected one, $(Li_{0.50}Na_{0.35})CoO_2$, and its structure, confirmed by Rietveld refinement of the XRD pattern, presents an ideal alternate ordering of lithium, cobalt, and sodium layers within OP4-type oxygen packing. The presence of vacancies in both alkali-ion layers was confirmed by electrochemical intercalation of lithium and sodium. For the first time, a new type of layered oxide exhibiting OPP9-type oxygen packing was evidenced. Between the CoO_2 slabs, alkali ions are intercalated in the following order: Li_{octa}−Na_{prism}−Na_{prism}. This material crystallizes in the $R\bar{3}m$ space group with a_{hex} = 2.828 Å and c_{hex} = 46.85 Å cell parameters.

1. INTRODUCTION

Layered oxides A_xCoO_2 (A = Li, Na) attract much research interest because of their outstanding physical properties. They were first studied as positive electrodes for both sodium[1,2] and lithium[3] battery materials. $LiCoO_2$ is nowadays widely spread in commercial Li-ion batteries. More recently, the interest was focused more on the sodium compounds after Terasaki et al. extended a preliminary work about polycrystalline $Na_{\sim 0.7}CoO_2$[4,5] and reported the promising thermoelectric properties of a $Na_{\sim 0.7}CoO_2$ single crystal,[6] which was later generalized for sodium-richer compositions ($x > 0.7$).[7,8] The discovery of superconductivity in hydrated sodium phases further demonstrated the extraordinary behavior in this family of materials.[9,10]

The lamellar structure is the key point to explaining such a wide range of peculiar properties: it consists of a stacking of edge-shared CoO_6 octahedral layers forming CoO_2 slabs between which alkali ions are intercalated. Depending on the nature of the A element, its content (x), and the synthesis conditions, different intercalation site symmetries are available in the interslab space: octahedral sites like those in Li_xCoO_2[11] and $NaCoO_2$,[12] trigonal-prismatic sites in Na_xCoO_2 or K_xCoO_2,[12−15] and tetrahedral sites in deintercalated bilayered $LiCoO_2$.[16] In order to simplify the description of the structure and highlight the stacking sequence, a specific nomenclature, used all along this report, was proposed where a letter qualifies the A cation environments and a figure gives the number of required CoO_2 layers in the hexagonal cell (e.g., O3-$LiCoO_2$ for the α-$NaFeO_2$-type lithium−cobalt double oxide).[17]

In 1994, Balsys and Lindsay Davis first reported the synthesis of a mixed lamellar oxide, $Li_{0.43}Na_{0.36}CoO_2$, prepared by heating an equimolar mixture of P2-$Na_{\sim 0.7}CoO_2$ and O3-$LiCoO_2$.[18] Their initial precursor's ratio was, however, not optimized, and some O3-$LiCoO_2$ remained in the final product. From a neutron powder diffraction study, they performed the only structural determination reported until now and especially noticed that the alkali ions keep their original intercalation site symmetry, i.e., nearly octahedral (D_{3d}) and trigonal prismatic (D_{3h}) for the Li and Na ions, respectively.

This implies that the two different alkali ions occupy discrete layers; these authors evidenced their ordering along the c axis in alternating layers (Figure 1). Note that there are two kinds of Na-ion sites, depending on whether the NaO_6 prism shares faces (Na_1 or Na_f) or edges (Na_2 or Na_e) with surrounding CoO_6 octahedra, as was already observed in the P2 stacking. According to their work, this compound crystallizes in the $P6_3mc$ space group with a_{hex} = 2.839(4) Å and c_{hex} = 20.36(3) Å. It is, to our knowledge, the only reported ordered (A/A′)MO_2-layered oxide.

Later Cao and co-workers extended this first work by directly mixing lithium and sodium carbonates and cobalt oxide in various proportions.[19,20] From a unique precise ratio, they obtained a pure compound with the chemical composition $Li_{0.48(1)}Na_{0.35(1)}CoO_2$ [determined by inductively coupled plasma atomic emission spectrometry (ICP-AES)] that has cell parameters similar to those reported by Balsys and Lindsay Davis.[18] For their structural analysis, they used the $P6_3/mmc$ space group, without further discussing their proposition. Following the above-mentioned nomenclature,[17] they labeled this stacking OP4. They used a slightly higher synthesis temperature (900 °C instead of 850 °C) and sometimes reported the presence of cobalt oxide traces in their final products. They also noticed that a fast cooling after thermal treatment improves their result, however, without proposing any explanation for this. They performed physical measurements on sintered pellets and reported at room temperature an enhanced thermopower (180 $\mu V \cdot K^{-1}$) compared that of P2−$Na_{\sim 0.7}CoO_2$ and both low electrical resistivity (∼30 mΩ·cm) and thermal conductivity (∼2 $W \cdot m^{-1} \cdot K^{-1}$), which offers an incentive figure of merit of $ZT = 3 \times 10^{-2}$.

Received: November 4, 2010
Published: February 18, 2011

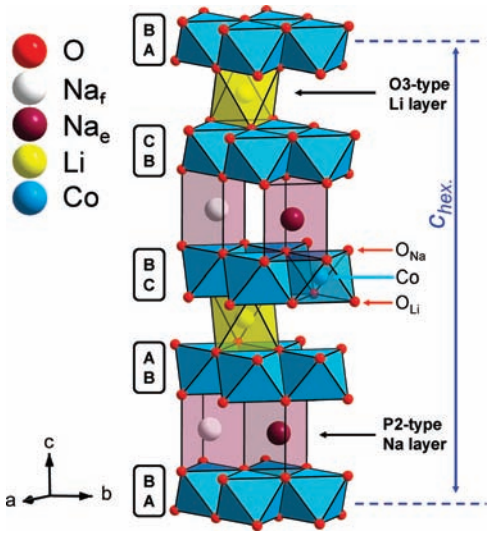

Figure 1. Perspective representation of OP4-(Li/Na)CoO_2. Li ions (in yellow) accommodate octahedral sites, while Na ions can occupy two kinds of trigonal-prismatic sites depending on whether they share faces (Na_f, in white) or edges (Na_e, in purple) with surrounding CoO_6 octahedra. The successive O-atom positions are labeled with the letters A, B, and C, which stand for the three available triangular lattices in a close-packed lattice. In the $P6_3/mmc$ space group, there are two distinct O atoms, O_{Na} and O_{Li}, which only differ by the nature of the closest alkali layer.

In 2007, Bos et al. explored sodium and lithium chemical deintercalation from an initial $Li_{0.41}Na_{0.31}CoO_2$ phase, obtained with Cao's protocol, and noticed decreasing thermoelectric properties for lower alkali content.[21] More recently, Semenova et al. also studied this compound using Raman spectroscopy and confirmed the presence of both O3-$LiCoO_2$ and P2-Na_xCoO_2 layers in the OP4 structure.[22] Finally, in 2009, both our group and Komaba et al. simultaneously used this phase as a precursor for a Na^+/Li^+ ionic exchange to prepare the new O4-$LiCoO_2$ polytype.[23,24]

In the present paper, we focus on this ordered OP4 phase and reinvestigate its synthesis mechanism and thermal stability using in situ X-ray diffraction (XRD) experiments. The chemical composition is also discussed. Additionally, the study was also extended to the whole $Na_{\sim 0.7}CoO_2-LiCoO_2$ system.

2. EXPERIMENTAL SECTION

2.1. Synthesis of the Precursors. Raw materials O3-$LiCoO_2$ and P2-$Na_{\sim 0.7}CoO_2$ are obtained from solid-state reactions using dry alkali carbonates and cobalt oxide Co_3O_4 precursors that are intimately ground. A stoichiometric ratio is used for the preparation of $LiCoO_2$, while an excess of 5 wt % sodium carbonate is added for the preparation of $NaCoO_2$ in order to balance the sodium volatility at high temperature. These mixtures are respectively heated at 900 and 850 °C for 24 h under an oxygen flow, with heating and cooling rates set at +2 and −5 °C·min^{-1}, respectively. In order to avoid moisture contamination, the final products were kept in an argon-filled glovebox.

2.2. Sample Characterization. XRD characterization was performed using a PANalytical X'Pert Pro powder diffractometer in the Bragg−Brentano geometry using Co Kα radiation. Data were collected through an X'Celerator detector in variable 2θ ranges (5−120° for Figure 5 and 3−100° for Figure 11). in situ experiments were carried out in an Anton-Paar HTK 1200N oven chamber under a dry oxygen flow. Thermal sequences consisted of heating and cooling steps with regular stabilization periods, during which XRD acquisitions were collected. For these experiments, the collection window was reduced to the 2θ range 18−26° to focus on the (00l) main diffraction peaks of each layered compound.

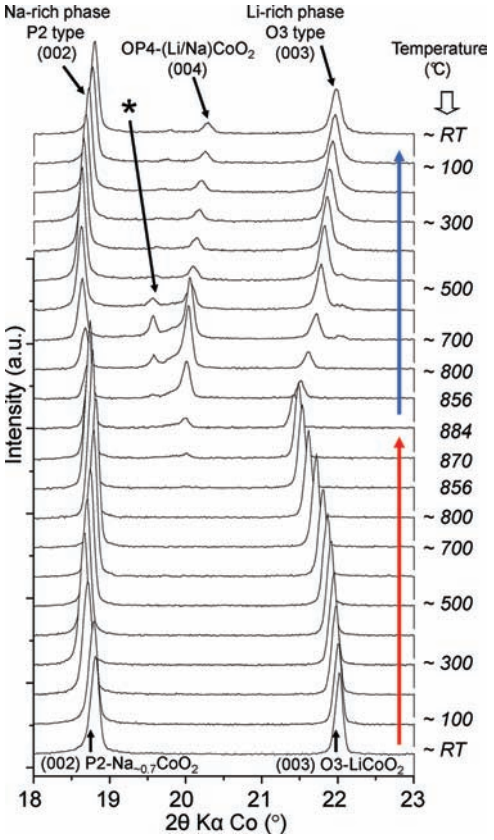

Figure 2. in situ XRD pattern evolution vs temperature for an initial equimolar ratio of O3-$LiCoO_2$ and P2-$Na_{\sim 0.7}CoO_2$ showing formation of the ordered OP4-(Li/Na)CoO_2 compound at high temperature. The cooling sequence down to 100 °C evidences its instability with the retrieval of both sodium-rich P2 and lithium-rich O3 compounds. The peak marked with an asterisk refers to the 1:2 ordering (thermal treatment parameters: mean rate ±∼1 °C·min^{-1}; acquisitions of ∼9 min every 14 °C at stabilized temperature; for clarity, only one pattern over six is shown).

Electrochemical intercalations of Na or Li ions were performed using the OP4 phase as the active material of the positive electrode of sodium or lithium batteries. In both cases, the material was mixed with carbon black (to enhance the electronic conductivity) and poly(tetrafluoroethylene) as a binder in a 87:10:3 mass ratio. The negative electrode was respectively metallic sodium or lithium for the sodium or lithium batteries; the liquid electrolyte was a $NaClO_4$ (1 M) solution in propylene carbonate for sodium batteries and $LiPF_6$ (1 M) in ethylene carbonate/propylene carbonate/dimethyl carbonate (1:1:3) for lithium batteries. Airtight cells were assembled in a drybox under an argon atmosphere to avoid moisture contamination. Galvanostatic modes with the cycling rate set to C/100 were used.

2.3. Stacking Defect Simulations. XRD pattern simulations were performed with the *DIFFaX* program developed by Treacy et al. in order to determine how the stacking faults involving excess sodium layers may alter the XRD patterns.[25] Various amounts of defects were tested from 0 to 100% with a 5% step. Co $K\alpha_1$ radiation was chosen in order to compare simulations with experimental XRD patterns.

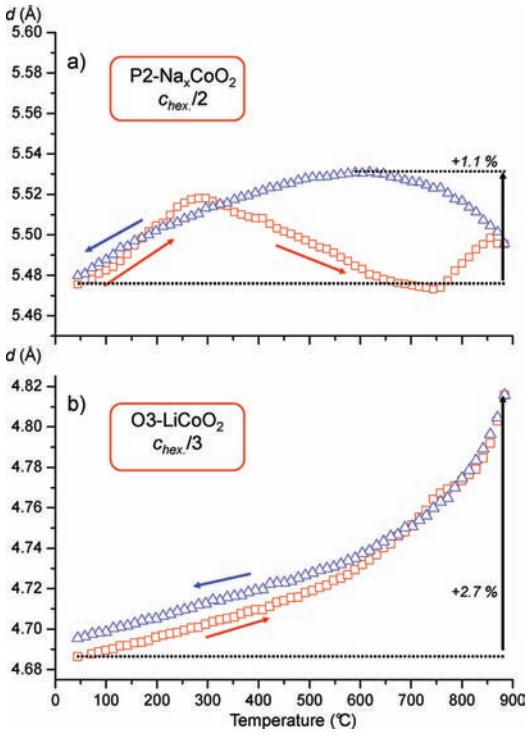

Figure 3. Evolution of the *d* parameter of (a) P2-Na_xCoO_2 and (b) O3-$LiCoO_2$ determined from the in situ experiment during formation and decomposition of the (Li/Na)CoO_2-ordered phases (OP4 mainly and OPP9; cf. Figure 3). Red squares and blue triangles stand for heating and cooling sequences, respectively. The uncertainty of the *d* parameter is always lower than 10^{-3} Å.

3. RESULTS AND DISCUSSION

3.1. in situ XRD Experiments. Several authors have reported on the synthesis of the OP4-(Li/Na)CoO_2 compound[18−21] with some nuances in the synthesis protocol, and most of them agree on the difficulty to obtain a pure phase. Our attempts to reproduce some of these works were unsuccessful. Although the OP4-(Li/Na)CoO_2 phase was always obtained, some O3-$LiCoO_2$ and/or P2-$Na_{\sim 0.7}CoO_2$ always remained in the final product. in situ XRD experiments were done to reinvestigate the synthesis of the OP4 compound and identify the origin of these results. In the first step, the experiment was carried out from an initial mixing of O3-$LiCoO_2$ and P2-$Na_{\sim 0.7}CoO_2$ in an equimolar ratio like that in the work of Balsys and Lindsay Davis.[18]

Figure 2 shows the XRD patterns collected for temperatures ranging from room temperature to 884 °C. There is no reaction between the two precursors before ∼856 °C, and only highest temperature patterns evidence the growth of the (004) diffraction peak of the ordered OP4-(Li/Na)CoO_2 phase at $2\theta \sim 20.0°$. Its formation continues until ∼884 °C (i.e., the highest temperature reached in this experiment) and even during the beginning of the cooling sequence (above ∼800 °C) because of the slow kinetics of the reaction. It should be noted that for this in situ study the sample stays only roughly 70 min above 850 °C, which is significantly less than that in the reported synthesis (4 days at 850 °C[18] or 30 h at 900 °C[19]). Such a short duration was chosen to prevent any decomposition of the product in the XRD high-temperature chamber, as preliminary experiments performed with a longer high-temperature

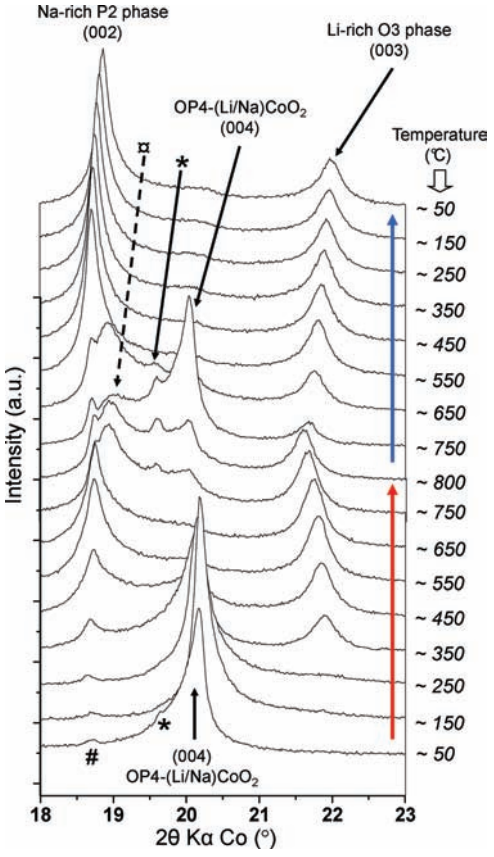

Figure 4. in situ XRD pattern evolution vs temperature for an almost pure OP4-(Li/Na)CoO_2 compound showing its decomposition from ∼350 to ∼750 °C into P2 sodium-rich and O3 lithium-rich compounds that further recombine. The 1:2 ordered compound already present in the initial product (see the left tail of the OP4 diffraction peak marked with an asterisk) follows the same steps. The hump marked with # corresponds to a P2-$Na_{\sim 0.7}CoO_2$ residual phase (thermal treatment parameters: mean rate ±∼0.3 °C·min^{-1}, acquisitions of ∼9 min every 25 °C at stabilized temperature; for clarity, only one pattern over four is shown). The peak (*) corresponds to the OPP9 stacking; the origin of the peak (⊙) is still undetermined.

treatment systematically evidenced the presence of cobalt oxide.

The asymmetry of the (004) diffraction peak with a tail at low angle can result from the presence of stacking faults, like those already reported in nickel hydroxides.[26] Simultaneously with the (004) peak, another peak appears at $2\theta = 19.6°$; it is identified as the (009) peak of a new alternate-layered phase, which will be considered hereafter. During the cooling step (−1 °C·min^{-1} without quenching), the intensities of both alternate-ordered-phase diffraction peaks slightly decrease, while in parallel, the intensities of both P2-Na_xCoO_2 and O3-$LiCoO_2$ diffraction peaks increase.

All along this experiment (even at the maximum of the ordered phase formation, i.e., at 800 °C during the cooling step), both P2 and O3 precursors remain present. Following the 2θ shift for their respective (00*l*) diffraction peak during the in situ experiment, the evolution of their c_{hex} parameter can be observed. In order to better compare the behavior of the two precursors, Figure 3 gathers the evolution of one $ACoO_2$ block thickness (named *d* hereafter) that directly corresponds to the combined thicknesses of one CoO_2 slab and one AO_2 interslab (A = Li, Na).

dx.doi.org/10.1021/ic102218w |*Inorg. Chem.* 2011, 50, 2420–2430

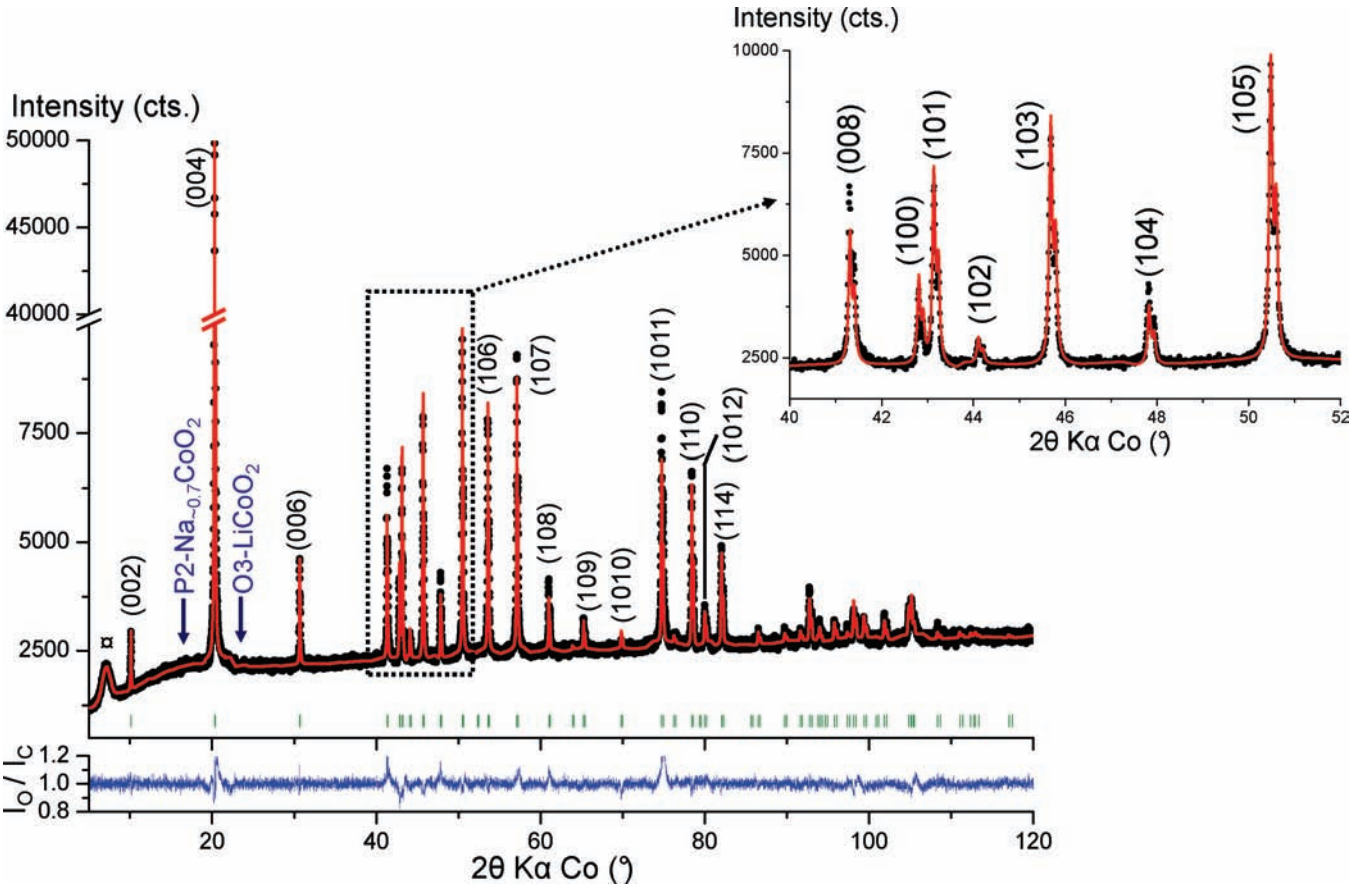

Figure 5. Experimental powder XRD pattern of the purest OP4-(Li/Na)CoO_2 obtained after synthesis with the optimized protocol (see the text). As evidenced by the blue arrows, the final product does not contain any trace of the P2 and O3 precursors. The observed (black points), calculated with Rietveld refinement (red line), and relative difference (bottom blue line, without unit) profiles, as well as Bragg position (vertical bars), are shown. The hump marked by # is due to the polymer window of the airtight cell. The inset evidences the good quality of the refinement despite some intensity peak errors, with especially a good matching in the diffraction peak shape.

Table 1. Rietveld Refinement Result on the OP4-(Li/Na)CoO_2 Powder Sample (Corresponding XRD Pattern in Figure [5]) with Space Group $P6_3/mmc$[a]

atom	site	x	y	z	occupancy	B (Å^2)
Co	4f	$^2/_3$	$^1/_3$	0.3838(0)	1	0.10(1)
Na_f	2d	$^2/_3$	$^1/_3$	$^1/_4$	0.240(0)	0.10(1)
Na_e	2c	$^1/_3$	$^2/_3$	$^1/_4$	0.516(0)	1.04(1)
Li	2a	0	0	$^1/_2$	0.84	0.2
O_{Li}	4f	$^1/_3$	$^2/_3$	0.4335(1)	1	0.15(1)
O_{Na}	4e	0	0	0.3395(1)	1	0.10(1)

a_{hex} = 2,8301(2) Å — c_{hex} = 20,286(2) Å

Pseudo−Voigt function PV = $\eta L + (1 - \eta)G$ with $\eta = \eta_0 + X(2\theta)$ — η_0 = 0.978(2) and X = 0.004(2)

profile parameters — U = 0.019(6); V = −0.006(5); W = 0.005(2)

R_p = 2.49, R_{wp} = 3.75, R_{exp} = 1.89 — χ^2 = 3.96

cR_p = 39.0, cR_{wp} = 21.0, cR_{exp} = 10.54 — R_{Bragg} = 17.3

[a] Standard deviations are multiplied by the S_{cor} number (5.6) to correct for local correlations.

Note that in both cases the c_{hex} parameter results from this d value multiplied by the number of CoO_2 slabs within the hexagonal cell.

For the O3-$LiCoO_2$ phase, the d parameter increases during heating to the highest temperature (884 °C) and then decreases during the cooling sequence (Figure 3b). The increase reaches

dx.doi.org/10.1021/ic102218w |*Inorg. Chem.* 2011, 50, 2420–2430

Table 2. Comparison of Experimental Crystallographic Data of $Li_{0.42}Na_{0.37}CoO_2$ and Those Recalculated from $Li_{0.43}Na_{0.36}CoO_2$[18] and Its Two Parent Phases (Data from References 11 and 13)

	P2-$Na_{0.74}CoO_2$ (Balsys and Davis[13])	$Li_{0.42}Na_{0.37}CoO_2$ (this work)	$Li_{0.43}Na_{0.36}CoO_2$ (Balsys and Lindsay Davis[18])	O3-$LiCoO_2$ (Levasseur et al.[11])
		Space Group		
	$P6_3/mmc$	$P6_3/mmc$	$P6_3mc$	$R\bar{3}m$
		Lattice Parameter (Å)		
a_{hex}	2.840(1)	2.8301(2)	2.839(4)	2.8143(2)
c_{hex}	10.811(1)	20.286(2)	20.36(3)	14.049(1)
		Atomic Distance (Å)		
Co−Co	2.840(1)	2.8301(2)	2.839	2.8143(2)
$Co-O_{Na}$	(×6) = 1.914	(×3) = 1.865(1)	1.859/1.973	
$Co-O_{Li}$		(×3) = 1.931(1)	1.999/1.882	(×6) = 1.921
$Li-O_{Li}$		(×6) = 2.107(1)	2.111	(×6) = 2.091
$Na-O_{Na}$	(×6) = 2.373	(×6) = 2.442(3)	2.390	
		Slab and Interslab Thicknesses (Å)		
CoO_2	1.975	1.906(1)	2.022	2.049
NaO_2	3.431	3.631(1)	3.477	
LiO_2		2.700(1)	2.659	2.633

Table 3. $ACoO_2$ (A = Li, Na) Block Definition Used To Build the OP4 Stacking and To Simulate the XRD Pattern with the *DIFFaX* Program[a]

layer	atom	x	y	z	occupancy
1	Na_e	$^2/_3$	$^1/_3$	0.138	0.516
	Na_f	0	0		0.240
	O	$^1/_3$	$^2/_3$	0.045	1
	Co	0	0	0	1
	O	$^2/_3$	$^1/_3$	−0.045	1
2	Na_e	$^1/_3$	$^2/_3$	0.138	0.516
	Na_f	0	0		0.240
	O	$^2/_3$	$^1/_3$	0.045	1
	Co	0	0	0	1
	O	$^1/_3$	$^2/_3$	−0.045	1
3	Li	$^1/_3$	$^2/_3$	0.116	0.84
	O	$^2/_3$	$^1/_3$	0.045	1
	Co	0	0	0	1
	O	$^1/_3$	$^2/_3$	−0.045	1
4	Li	$^2/_3$	$^1/_3$	0.116	0.84
	O	$^1/_3$	$^2/_3$	0.045	1
	Co	0	0	0	1
	O	$^2/_3$	$^1/_3$	−0.045	1

[a] The z-reduced coordinates are calculated to match the slab and interslab thicknesses found in Table 2.

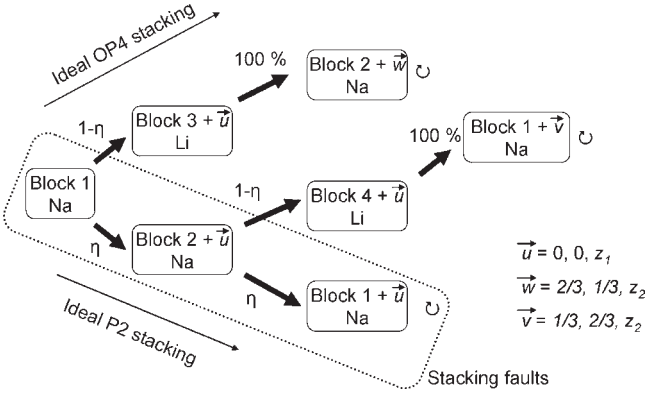

Figure 6. Schematic representation of the $ACoO_2$ (A = Li, Na) block succession from an ideal OP4 structure (top, $\eta \neq 0$) to a pure P2-type sodium stacking (bottom, $\eta \neq 1$). In the OP4 configuration, each $NaCoO_2$ block is followed by a $LiCoO_2$ one and vice versa. Stacking defects are induced by some $NaCoO_2$ blocks that sporadically replace a lithium one. Repeatable sequences are marked with the clockwise symbol.

2.7% of the initial value. This tendency is globally related to thermal expansion of the compound. The final d value is slightly higher than the one at the beginning of the experiment. Understoichiometric Li_xCoO_2 phases (with $x \leq 1$) are characterized by higher c_{hex} parameters,[27] but their presence here is discarded because such compositions can only be obtained by electrochemical or chemical deintercalation, while the solid-state route never leads to understoichiometric phases.[3,28,29] Here, the larger d value for O3-$LiCoO_2$ appears upon cooling of the sample below 700 °C, when O3-$LiCoO_2$ is formed again from decomposition of the OP4-$(Li/Na)CoO_2$ phase. We suggest that some sporadic sodium layers might remain and lead to an overall O3-$(Li_{1-\varepsilon}Na_\varepsilon)CoO_2$ phase with an artificially (by defects) increased d parameter. This assumption is supported by the slight broadening of the diffraction peak [the full width at half-maximum (fwhm) was 0.15° at the end of the experiment, while it was 0.11° at the beginning].

For the sodium phase, the evolution is weaker when the highest increase is only +1.1% (Figure 3a). The general evolution of the d parameter accounts for a more complex behavior, which is not yet understood but, however, might be ruled by different factors depending on the temperature range. Below 300 °C, the standard thermal expansion effect tends to increase the parameter. The abrupt drop between 300 and 700 °C is more difficult to explain, but it might be due to the

dx.doi.org/10.1021/ic102218w |*Inorg. Chem.* 2011, 50, 2420–2430

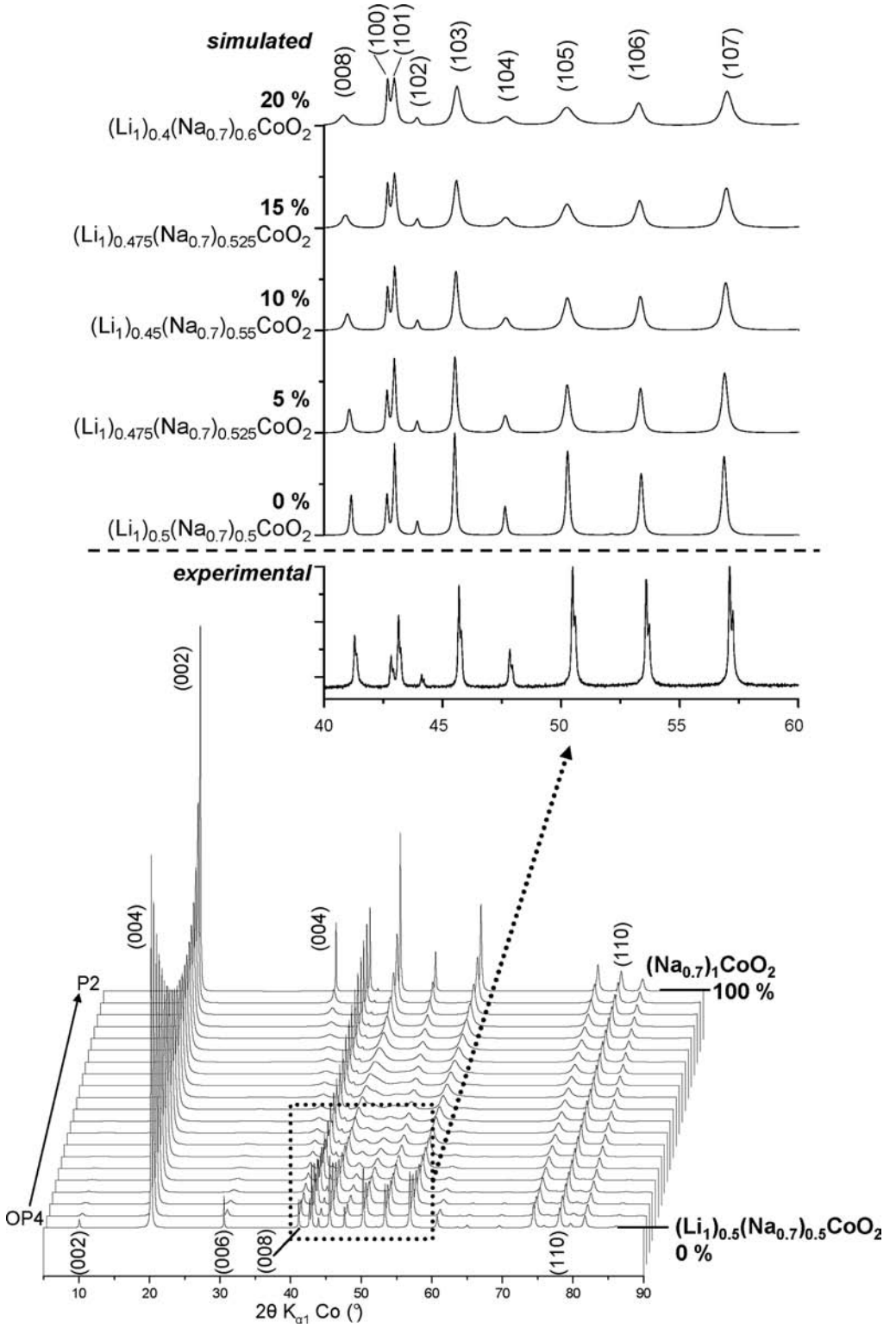

Figure 7. Simulated XRD patterns calculated with the *DIFFaX* program from an ideal OP4 packing scheme (η = 0) to a 100% faulted structure corresponding to P2 stacking (η = 1), with a step of 5%. η represents the defect probability factor. The inset compares in the 40−60° 2θ range the experimental pattern with the simulated ones with different amounts of defects.

very beginning of intercalation of the lithium layers in the interslab space. After 750 °C, composition changes due to interactions with the OP4 phase formation may explain the second increase of the *d* parameter that continues in the beginning of the cooling sequence. Thermal contraction in the final step down to room temperature leads to the observed regular decrease of the *d* parameter.

No pertinent information could be obtained from the evolution of fwhm versus temperature for the (002) peak: it simply behaves like a random variable and roughly follows a normal

dx.doi.org/10.1021/ic102218w |*Inorg. Chem.* 2011, 50, 2420–2430

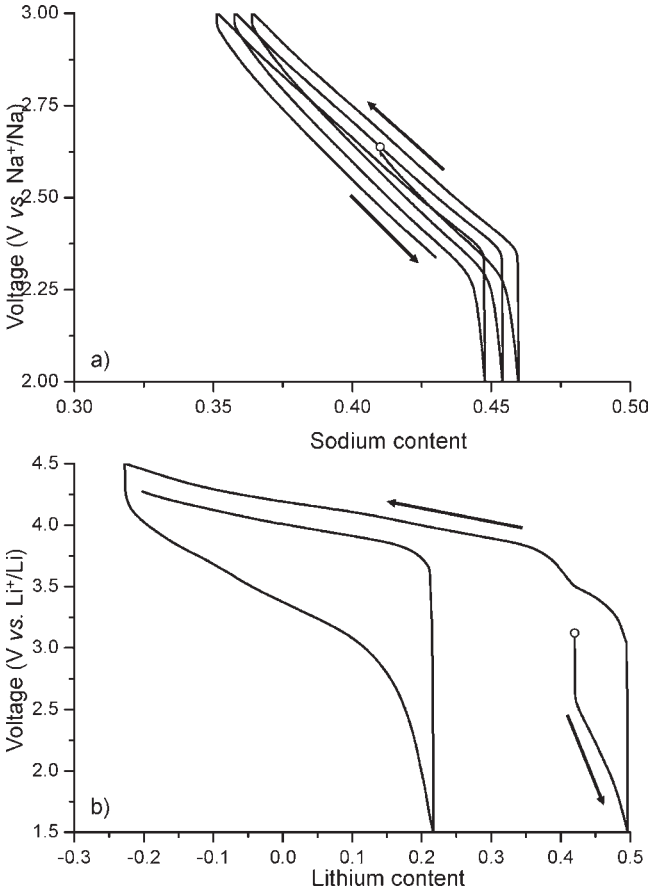

Figure 8. Electrochemical cycling curves of sodium (a) and lithium (b) batteries with the OP4 phase as the active material of the positive electrode. In both cases, the first discharge evidences the unfilled alkali interslab spaces. Starting points in white circles are set to 0.41 and 0.42 for sodium and lithium batteries, respectively, according to the nominal composition $Li_{0.42}Na_{\sim 0.41}CoO_2$.

distribution without any direct link with the temperature. For this compound, also the initial c_{hex} value is not recovered; it slightly increases, as expected, from a more sodium-deficient compound.[1]

In parallel with the (004) diffraction peak of the OP4 phase, another peak that does not belong to any of the considered phases appears at high temperature (at lower angle, $2\theta \sim 19.5°$) and then tends to vanish during the slow cooling step. At such a high temperature, moisture effects that often lead to a high c_{hex} lattice parameter (as in the hydrated superconductive phase[9,10]) are impossible here. This peak is, in fact, the (009) diffraction line of a new (Li/Na/Na)CoO_2 phase with OPP9 oxygen stacking, which will be detailed hereafter.

A second in situ XRD experiment was performed by heating to ~800 °C an almost pure OP4-(Li/Na)CoO_2 sample (weak initial presence of P2-Na_xCoO_2) in order to clarify its high-temperature thermal stability. As shown in Figure 4, the intensity of the (004) diffraction peak begins to decrease between 250 and 350 °C, while two peaks arising from a P2 sodium-rich compound on the one side ($2\theta \sim 18.6°$) and an O3 lithium-rich compound on the other side ($2\theta \sim 22°$) appear. For both P2 and O3 phases obtained after cooling, the asymmetric shape of the diffraction peaks results from nonideal structures, while the width broadening (fwhm values at ~650 °C: 0.42° and 0.34°, respectively) may be explained by the small size of the grains, which are formed at

Table 4. Expected Crystallographic Data of the Ordered OPP9-(Li/Na/Na)CoO_2 Stacking Based on Experimental Data of P2-$Na_{\sim 0.7}CoO_2$[14] and O3-$LiCoO_2$[11]

	P2-$Na_{\sim 0.7}CoO_2$	O3-$LiCoO_2$	ordered stacking OPP9-(Li/Na/Na)CoO_2
a_{hex} (Å)	2.8314(9)	2.8143(2)	2.826[a]
c_{hex} (Å)	10.8756(4)	14.049(1)	46.677[b]
AO_2 interslab thickness (Å)	3.471	2.633	3.471[c]
			2.633[c]
CoO_2 slab thickness (Å)	1.967	2.049	1.967[d]
			2.008[e]

[a] Obtained from the P2 and O3 average. [b] Obtained in the *P*1 space group and valid for the $R\bar{3}m$ space group (hexagonal system). [c] Assumed similar to the initial P2 and O3 compounds. [d] CoO_2 slab surrounded by two NaO_2 layers. [e] CoO_2 slab surrounded by one NaO_2 and one LiO_2 layer, obtained from the P2 and O3 average.

Table 5. Atomic Positions of the OPP9-(Li/Na/Na)CoO_2 Phase (Space Group $R\bar{3}m$) Based on the Stacking Simulation[a]

atom	site	*x*, *y*, *z*	occupancy
Co1	1a	0	1
Co2	2c	0.883	1
Li	1b	$^1/_2$	
Na_f	2c	0.058	
Na_e	2c	0.725	
O1	2c	0.355	1
O2	2c	0.429	1
O3	2c	0.805	1

[a] Alkali site occupancies are not given; however, by analogy with the OP4 compound that exhibits sodium and lithium unfilled layers, the occupancy factors might also be less than 1 for the OPP9 phase. Like in the P2-$Na_{\sim 0.7}CoO_2$ precursor, Na ions can occupy two different sites depending on whether the prisms share only edges (Na_e) or faces (Na_f) with the surrounding CoO_6 octahedra.

a temperature sensibly lower than the ones used for the conventional synthesis of these phases (see section 2).

The decomposition during the heating sequence stops near 750 °C with a nearly full disappearance of the OP4-(Li/Na)CoO_2 compound, which begins to grow again above 750 °C from the sodium- and lithium-rich decomposition products. Such early growth compared to the first experiment (~800 °C) is most probably related to an improved reactivity of the precursors because of both smaller grain size and more intimate mixing.

In the 650−800 °C temperature range, a very complex behavior is observed with the appearance and disappearance of the diffraction peak due to the above-mentioned OPP9 phase, which is already present in the starting material, while another peak around $2\theta \sim 19°$ appears and disappears in the same range. It may be related to another Li/Na stacking that has not yet been characterized or to another P2-type phase with different sodium content. Indeed, during the cooling sequence, the two peaks close to $2\theta \sim 19°$ tend to merge as a homogenization of the system; the group of Alloul used this latter process with mixtures of $Na_{1/2}CoO_2$ and $Na_{0.71}CoO_2$ compounds to obtain homogeneous products with controlled sodium content.[30]

dx.doi.org/10.1021/ic102218w |*Inorg. Chem.* 2011, 50, 2420–2430

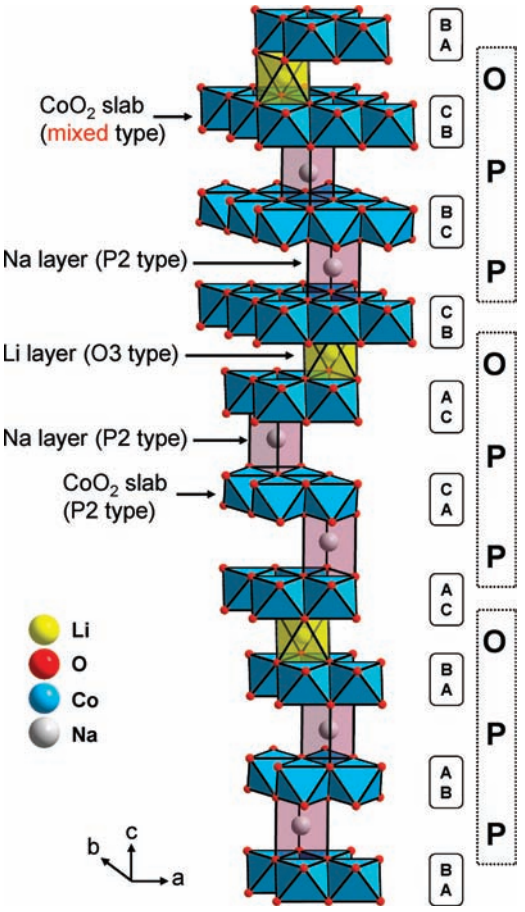

Figure 9. Perspective representation of the ordered OPP9-(Li/Na/Na)CoO_2 stacking. The successive O-atom positions are labeled with the letters A, B, and C, which stand for the three available triangular lattices in a close-packed lattice, while letters P and O refer to the alkali ion environments. Na ions accommodate NaO_6 trigonal prisms (in pink), while Li ions occupy LiO_6 octahedra (in yellow), just like in the case of the OP4 packing (Figure 1). For clarity, among the two kinds of Na ions available in this stacking (Na_f and Na_e), only the latter is here represented.

This in situ study underlines the instability of the OP4 phase, which tends to decompose during both low cooling and heating sequences. Thermal treatment in a preheated furnace and with a fast final quench can impede decomposition.

3.2. Modified Protocol of the Synthesis. Following these observations, the synthesis protocol was slightly tuned; the main points are as follows: (i) the heating rate is maximized by directly putting the precursors in a preheated furnace; (ii) the product is quenched from high temperature to avoid its decomposition during the cooling step and, consequently, (iii) the reaction is made in a gold-sealed tube to allow plunging of the sample in a water bath at the end of thermal treatment; (iv) with the atmosphere being closed, the precursors are carbonate-free and the layered oxide O3-$LiCoO_2$ and P2-$Na_{\sim 0.7}CoO_2$ precursors are used like in the initial work of Balsys and Lindsay Davis.[18] The use of a sealed tube also prevents Na_2O departure. These precursors are ground together in a glovebox in the molar ratio of 42:58 and then enclosed in the gold-sealed tube that is directly put into a furnace preheated at 920 °C; it is kept inside for 24 h before the final quench. After quenching, the final product is stored in a dry atmosphere.

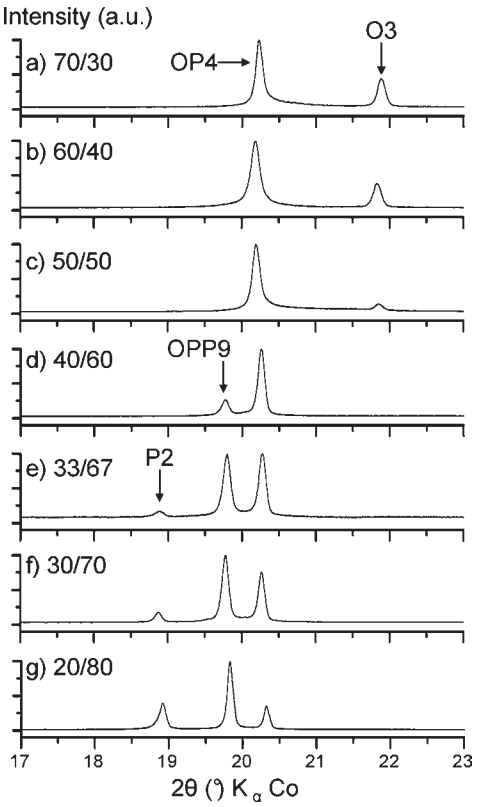

Figure 10. Experimental XRD patterns obtained from various reacted mixtures of O3-$LiCoO_2$ and P2-$Na_{\sim 0.7}CoO_2$. The initial ratios are given near the patterns. XRD patterns exhibit the main diffraction peaks of O3 and OP4 (a−c), OP4 and OPP9 (d), and OP4, OPP9, and P2 (e−g). The positions of the ordered phase (OP4 and OPP9) diffraction peaks do not change from one nominal ratio to another, implying a constant alkali content in the compounds.

The precise ratio 42:58 was found empirically and may slightly vary depending on the real sodium content of the P2-$Na_{\sim 0.7}CoO_2$ batch. It was indeed found that the global initial sodium content of the precursor, which can slightly vary around 0.7 from one synthesis to another, largely influences the purity of the final product and is thus a very critical parameter to the obtention of a pure OP4 phase. Note that the ideal ratio 42:58 matches with an equimolar content of lithium and sodium in the initial mixture and corresponds to the chemical formulas $Li_{0.42}Na_{\sim 0.41}CoO_2$. Although the heating temperature is higher than that in previous works, the closed atmosphere in the gold-sealed tube seems to prevent sodium oxide departure and, therefore, formation of cobalt oxide.

3.3. OP4 Phase Characterization. *Structural Refinement.* The experimental XRD pattern shown in Figure 5 evidences completion of the reaction, with especially the absence of the main diffraction peaks of the precursors. In addition, no impurity is observed. The full pattern profile matching leads to refined hexagonal cell parameters [a_{hex} = 2.8296(1) Å and c_{hex} = 20.291(2) Å] in total agreement with the literature.[19,21]

Two different space groups, $P6_3mc$ and $P6_3/mmc$, were proposed in the previous studies.[18,19] As shown in Figure 1, the symmetry of the packing of each alkali plane (lithium and sodium) along the *c* axis, with a similar environment (successively oxygen−cobalt−oxygen planes), suggests using the more symmetric space group $P6_3/mmc$. In this case, only two O ions

dx.doi.org/10.1021/ic102218w |*Inorg. Chem.* 2011, 50, 2420–2430

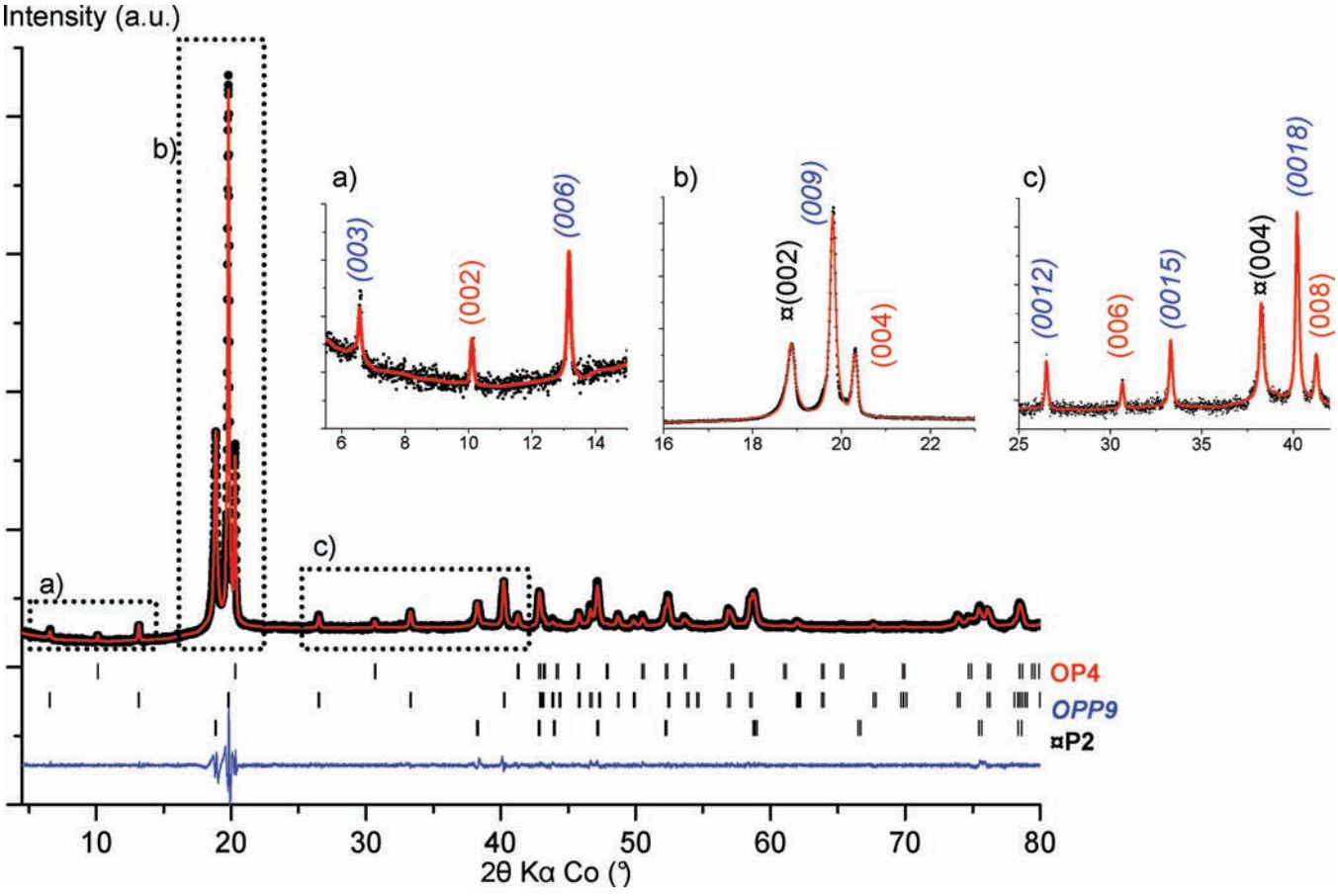

Figure 11. Experimental XRD pattern of a mixture of OP4, OPP9, and P2 phases obtained from a sodium-enriched nominal mixing (20:80 molar ratio; cf. Figure 9g). The observed (black points), calculated (solid red line), and difference (bottom blue line) profiles, as well as the Bragg positions (vertical bars), are shown. Below $2\theta = 42°$, the diffraction peak indexes are given: in italic blue for OPP9, in red for OP4, and in black for P2 (with the symbol ⌖ as the prefix).

(O_{Na} and O_{Li}) and one Co ion (in addition to the alkali ions) are necessary to describe the cell.

This latter space group was used in the present study to perform a structural refinement by the Rietveld method.[31] The occupancy factors of the Co and O ions were fixed to the nominal ones, while that for the Li ion (hardly seen in XRD) was fixed to 0.42, the expected value from the synthesis conditions. On the contrary, the Na-ion occupancies are refined. Table 1 summarizes the refined parameters. The resulting chemical composition $Li_{0.42}Na_{0.37}CoO_2$ agrees with that obtained from neutron diffraction by Balsys and Lindsay Davis[18] and leads, however, to a slightly lower amount of sodium compared to the nominal composition.

Table 2 compares the obtained crystallographic data with those calculated from the structural determinations reported for $Li_{0.43}Na_{0.36}CoO_2$,[18] $Na_{0.74}CoO_2$,[13] and $LiCoO_2$.[11] The main difference between the work of Balsys and Lindsay Davis and our refinement is the use of a lower symmetry by these authors. Note that this latter choice ($P6_3mc$) leads to the definition of two distinct Co sites that are refined separately. This implies the existence of different Co−O_A (A = Li, Na) distances, leading to a nonsymmetric environment for each alkali layer, without, however, any significant structural reason justifying such a result.

In our refinement, the unique Co−O_{Na} distance is shorter than the Co−O_{Li} one [where O_{Na} (respectively O_{Li}) stands for the O atom shared between the Co and Na (respectively Li) ions; cf. Figure 1]. This may be explained by the stronger ionic character of the Na−O_{Na} bond (especially when Na ions occupy prismatic sites[32]), which implies a strong covalent character of the antagonist Co−O_{Na} bond and shortens its length.

According to the refinement of Balsys and Lindsay Davis, the CoO_2 slab thickness seems to be intermediate between the ones of the parent phases (Table 2). Our refinement shows a global shrinkage of this slab associated to an increase of the NaO_2 and LiO_2 interslab spaces.

Discussion on the Chemical Composition: Simulation of the Stacking Faults. A strictly ideal OP4 stacking with alkali layers in the same kinds of interslab spaces as the parent phases $LiCoO_2$ and $Na_{\sim 0.7}CoO_2$ should have the chemical composition $Li_{0.5}Na_{0.35}CoO_2$. However, an equimolar ratio does not lead to formation of a pure ordered phase.[18] Moreover, the best results that we obtained came from the nominal ratio 42:58, for which the final chemical composition $Li_{0.42}Na_{0.37}CoO_2$, assuming the ideal OP4 packing, implies unfilled alkali layers.

This phenomenon is well-known in P2-type sodium phases, with especially the formation of Na^+/vacancy ordering for some peculiar compositions.[33−35] However, the composition is more unexpected as far as the lithium interslab filling is concerned because it is well-known that solid-state reactions of lithium−cobalt double oxides only lead to stoichiometric $LiCoO_2$. Keeping the hypothesis of completely filled lithium layers obviously involves an altered stacking of sodium and lithium layers, i.e., a long-range (1:1) order with some local

short-range disorder induced by an excess of P2-type sodium layers.

Following these remarks, we have studied the effect of such defects using XRD simulations with the *DIFFaX* program.[25] To describe the OP4 stacking, we have considered four $ACoO_2$ blocks, each made of one CoO_2 slab and one alkali layer (Na or Li) lying above (Table 3). Atomic positions correspond to the three available ones characteristic of a close-packed lattice. Each z position was calculated to fit with the crystallographic parameters found by our structural refinement. In the ideal OP4 stacking, $LiCoO_2$ and $NaCoO_2$ blocks alternate perfectly. In a faulted structure with P2-type sodium layers in excess, $NaCoO_2$ blocks sporadically replace $LiCoO_2$ ones in the overall packing (Figure 6). For each step, the a_{hex} parameter was balanced with the a_{hex} parameters from $Li_{0.42}Na_{0.37}CoO_2$[18] and $Na_{0.71}CoO_2$[14] according to a *pseudo* Vegard's law. Figure 7 presents the simulated patterns obtained, from an ideal OP4 stacking to a P2 sodium stacking (Figure 6) with regular increases (5%) of the sodium layers (10 and 20% of the stacking faults respectively correspond to $Li_{0.42}Na_{0.37}CoO_2$ and $Li_{0.42}Na_{\sim 0.41}CoO_2$ chemical compositions); the inset compares the experimental pattern with the faulted ones in the 40−60° 2θ range. Several points can be highlighted from these simulations: (i) the (002) and (006) peaks quickly disappear because they are characteristic of the superstructure arising from the Li/Na (1:1) ordering; (ii) the (004) and (008) peaks slightly shift to lower 2θ positions (because the increasing amount of sodium interslabs enhances the average d spacing) to progressively merge with the (002) and (004) peaks, respectively, of the P2 phase; (iii) the (110) peak is (only) weakly modified because of the light evolution of a_{hex} (less than 0.9%); (iv) the stacking faults induce a broadening of all (hkl) diffraction peaks (with $l \neq 0$). The experimental XRD pattern does not evidence any of these features with, in particular, intense (00l) peaks and narrow (10l) lines. This observation discards the assumption of stacking defects in the OP4 structure (in a significant amount) and strongly supports the presence of vacancies in both lithium and sodium interslab spaces.

This point is confirmed with tests on batteries; the electrochemical cycling curves of the sodium or lithium batteries with the OP4-$(Li/Na)CoO_2$ phase as the active material of the positive electrode are presented in Figure 8. For completely filled interslab spaces, the alkali content is 0.5. In both cases, the first discharge clearly evidences that Na and Li ions can be intercalated into the layered structure. With the reasonable assumptions that (i) Li ions cannot occupy prismatic intercalation sites and (ii) Na ions hardly enter the lithium interslab space during the electrochemical process because of the significant thickness difference, the alkali ions should enter the interslab spaces containing the same cation. At the end of lithium intercalation, the lithium interslabs are almost completely filled, like in the case of $LiCoO_2$,[36] while in the case of sodium intercalation, some vacancies remain in the sodium layers, as is always observed during discharge of the Na/P2-Na_xCoO_2 batteries[2,37] This means that both interslab spaces (lithium and sodium) of the initial OP4 precursor are not completely filled. The remaining curves of the electrochemical cycling show that the process seems to be significantly more reversible in the case of sodium. Note that for lithium batteries the electrolyte decomposition at high potential shifts the real lithium content and hinders the clear understanding of the electrochemical process.

3.4. New OPP9 Oxygen Packing with One Lithium Layer for Two Sodium Layers. The in situ XRD experiments have evidenced the formation of a second phase competing with the growth of the OP4 compound. Its main diffraction peak is located at $2\theta \sim 19.5°$ in Figures 2 and 4, between those of the OP4 and P2-$Na_{\sim 0.7}CoO_2$ phases. In this 2θ range, the diffraction lines are related to the c_{hex} parameter. From simple steric arguments, we have made the hypothesis of a new phase richer in sodium than the OP4. Numerical consideration shows that the 2θ position of this unknown diffraction peak refers to an average d spacing of ∼5.20 Å very close to $^2/_3[c_{\text{P2-Na}_{0.7}\text{CoO}_2}{}^{hex}/2] + {}^1/_3[c_{\text{O3-LiCoO}_2}{}^{hex}/3]$ calculated for a stacking of two sodium layers in trigonal-prismatic sites and one lithium layer in an octahedral environment alternating with CoO_2 slabs.

Following the phase simulation approach used to build the O4-$LiCoO_2$ polytype based on the O2 and O3-$LiCoO_2$ polytype characteristics,[23] the (Li/Na/Na) 1:2 stacking was built using the characteristics of individual CoO_2 slabs and LiO_2 and NaO_2 interslabs in the parent phases. The different layers were organized to match P2 and O3 packing for respectively the sodium and lithium subcells. Such a structure can be described using a trigonal $R\bar{3}m$ space group with hexagonal cell parameters $a_{hex} = {}^2/_3 a_{\text{P2-Na}_{\sim 0.7}\text{CoO}_2}{}^{hex.} + {}^1/_3 a_{\text{O3-LiCoO}_2}{}^{hex.} \approx 2.826$ Å and $c_{hex} = 3c_{\text{P2-Na}_{\sim 0.7}\text{CoO}_2}{}^{hex} + c_{\text{O3-LiCoO}_2}{}^{hex} \approx 46.68$ Å. The other crystallographic data are summarized in Tables 4 and 5. The use of the hexagonal setting highlights the stacking sequence with nine CoO_2 sheets forming three blocks of Li_{octa}-CoO_2−Na_{prism}-CoO_2−Na_{prism}-CoO_2 layers (Figure 9). Following the extended nomenclature described above, this new compound is named OPP9-$(Li/Na/Na)CoO_2$, hereafter simply referred to as OPP9.

In order to try to obtain this phase by direct synthesis, the O3-$LiCoO_2$−P2-$Na_{\sim 0.7}CoO_2$ phase diagram was revisited in the molar ratios range 70:30−20:80 by using the protocol designed for the synthesis of OP4-$(Li/Na)CoO_2$. Figure 10 shows a part of the experimental XRD patterns obtained from these sets of various initial proportions. The selected 2θ range (17−23°) enables one to focus on the (00l) main diffraction peaks of all of these layered compounds (P2, OPP9, OP4, and O3 going from low to high 2θ values). For lithium-rich mixtures (Figure 10a−c), the final XRD patterns exhibit two distinct peaks ascribed to O3-$LiCoO_2$ and OP4-$(Li/Na)CoO_2$ compounds. For proportions less than or equal to 40:60, the OPP9 diffraction peak appears (Figure 10d and further), and there is no longer a trace of O3-$LiCoO_2$. This peak grows regularly with an increase in the initial P2-$Na_{\sim 0.7}CoO_2$ amount; however, it was impossible to fully eliminate this precursor (Figure 10e−g). The XRD measurement with a larger 2θ window is shown in Figure 11 for the sample obtained from the initial ratio 20:80 (i.e., with the largest amount of the OPP9 phase). The profile-matching calculations with these data account well for the cell parameters already detailed for the OP4 phase and the ones for the new OPP9 phase [$a_{hex} = 2.828(1)$ Å and $c_{hex} = 46.85(1)$ Å] very close to the simulated ($a_{hex} = 2.826$ Å and $c_{hex} = 46.674$ Å; see Table 4). Insets a and c clearly highlight the additional c-axis superstructure peaks of the OPP9 stacking. No Rietveld refinement is given because the result is largely confused as a result of the presence of three phases, both contributing in the same 2θ regions (especially for $2\theta > 40°$). In addition, the alkali deficiency of each phase also hinders a detailed structural analysis.

Focusing on the competing formation of the two ordered compounds and the stacking sequence, which prevents any sheet gliding phenomena between OPP9 and OP4 packing schemes, we can reasonably assume that the OPP9 stacking is not an intermediate phase, from the structural point of view, between

dx.doi.org/10.1021/ic102218w |*Inorg. Chem.* 2011, 50, 2420–2430

the P2-Na_xCoO_2 and OP4 phases. This means that (at least) two alternate stackings are available for Na and Li cations at high temperature (1:1 and 1:2). Attempts to complete this series on the lithium-rich side do not evidence a possible 2:1 Li/Na stacking (Figure 10a−c).

4. CONCLUSION

The synthesis of the 1:1 Li/Na-stacked OP4-$Li_{0.42}Na_{0.37}CoO_2$ phase from a mixture of O3-$LiCoO_2$ and P2-$Na_{\sim 0.7}CoO_2$ (42:58 molar ratio) in a gold-sealed tube maintained at 920 °C for 24 h and then quenched leads to a pure material. This phase is metastable and decomposes by giving back its two precursors on either heating to 350 °C and low cooling. The $P6_3/mmc$ space group appears to be the more suitable one to describe this structure. Simulation of the stacking fault influence clearly avoids the assumption of local disorder and confirms the alternate ordering of the lithium and sodium layers. The hypothesis of unfilled alkali layers, which results from the chemical composition calculated from the structural refinement, is also supported by electrochemical battery discharges, which evidences the possibility of Li- or Na-ion intercalation.

During this study, a new 1:2 stacking, which alternates one lithium layer and two sodium ones, is evidenced. This new compound labeled OPP9-(Li/Na/Na)CoO_2 appears as a competitor of OP4-(Li/Na)CoO_2 because its growth begins roughly at the same temperature.

The cell parameters of this new material, which crystallizes in the $R\bar{3}m$ space group, were determined. However, more experiments are required to obtain the OPP9 phase.

AUTHOR INFORMATION

Corresponding Author
*E-mail: pollet@icmcb-bordeaux.cnrs.fr.

ACKNOWLEDGMENT

The authors want to thank J. Villot, S. Fourcade, and C. Denage for technical assistance, E. Lebraud and S. Pechev for XRD assistance, and the ANR OCTE and Région Aquitaine for financial support. CEA is also thanked for a scholarship to R.B. Concerning the use of the *DIFFaX* program, R.B. wants to thank L. Croguennec (ICMCB-CNRS) and especially M. Treacy (Arizona State University) for fruitful discussions.

REFERENCES

(1) Braconnier, J.-J.; Delmas, C.; Fouassier, C.; Hagenmuller, P. *Mater. Res. Bull.* **1980**, *15* (12), 1797.
(2) Delmas, C.; Braconnier, J.-J.; Fouassier, C.; Hagenmuller, P. *Solid State Ionics* **1981**, *3−4* (C), 165.
(3) Mizushima, K.; Jones, P.; Wiseman, P.; Goodenough, J. *Mater. Res. Bull.* **1980**, *15* (6), 783.
(4) Molenda, J.; Delmas, C.; Hagenmuller, P. *Solid State Ionics* **1983**, *9−10* (1), 431.
(5) Molenda, J.; Delmas, C.; Dordor, P.; Stoklosa, A. *Solid State Ionics* **1984**, *12* (C), 473.
(6) Terasaki, I.; Sasago, Y.; Uchinokura, K. *Phys. Rev. B: Condens. Matter Mater. Phys.* **1997**, *56* (20), R12685.
(7) Lee, M.; Viciu, L.; Li, L.; Wang, Y.; Foo, M.; Watauchi, S.; Pascal, R.; Cava, R.; Ong, N. *Nat. Mater.* **2006**, *5* (7), 537.
(8) Lee, M.; Viciu, L.; Li, L.; Wang, Y.; Foo, M.; Watauchi, S.; Pascal, R.; Cava, R.; Ong, N. *Phys. B: Condens. Matter* **2008**, *403* (5−9), 1564.
(9) Takada, K.; Sakurai, H.; Takayama-Muromachi, E.; Izumi, F.; Dilanian, R.; Sasaki, T. *Nature* **2003**, *422* (6927), 53.
(10) Schaak, R.; Klimczuk, T.; Foo, M.; Cava, R. *Nature* **2003**, *424* (6948), 527.
(11) Levasseur, S.; Ménétrier, M.; Suard, E.; Delmas, C. *Solid State Ionics* **2000**, *128* (1−4), 11.
(12) Fouassier, C.; Matejka, G.; Reau, J.-M.; Hagenmuller, P. *J. Solid State Chem.* **1973**, *6* (4), 532.
(13) Balsys, R.; Davis, R. *Solid State Ionics* **1997**, *93* (3−4), 279.
(14) Huang, Q.; Foo, M.; Pascal, R.; Lynn, J.; Toby, B.; He, T.; Zandbergen, H.; Cava, R. *Phys. Rev. B: Condens. Matter Mater. Phys.* **2004**, *70* (18), 184110.
(15) Blangero, M.; Decourt, R.; Carlier, D.; Ceder, G.; Pollet, M.; Doumerc, J.-P.; Darriet, J.; Delmas, C. *Inorg. Chem.* **2005**, *44* (25), 9299.
(16) Carlier, D.; Croguennec, L.; Ceder, G.; Ménétrier, M.; Shao-Horn, Y.; Delmas, C. *Inorg. Chem.* **2004**, *43* (3), 914.
(17) Delmas, C.; Fouassier, C.; Hagenmuller, P. *Phys. B+C (Amsterdam, Neth.)* **1980**, *99* (1−4), 81.
(18) Balsys, R.; Lindsay Davis, R. *Solid State Ionics* **1994**, *69* (1), 69.
(19) Ren, Z.; Shen, J.; Jiang, S.; Chen, X.; Feng, C.; Xu, Z.; Cao, G. *J. Phys.: Condens. Matter* **2006**, *18* (29), L379.
(20) Chen, X.; Xu, X.-F.; Hu, R.-X.; Ren, Z.; Xu, Z.-A.; Cao, G.-H. *Acta Phys. Sin.* **2007**, *56*, 1627.
(21) Bos, J.; Hertz, J.; Morosan, E.; Cava, R. *J. Solid State Chem.* **2007**, *180* (11), 3211.
(22) Semenova, A.; Kellerman, D.; Baklanova, I.; Perelyaeva, L.; Vovkotrub, E. *Chem. Phys. Lett.* **2010**, *491* (4−6), 169.
(23) Berthelot, R.; Carlier, D.; Pollet, M.; Doumerc, J.-P.; Delmas, C. *Electrochem. Solid-State Lett.* **2009**, *12* (11), A207.
(24) Komaba, S.; Yabuuchi, N.; Kawamoto, Y. *Chem. Lett.* **2009**, *38* (10), 954.
(25) Treacy, M.; Newsam, J.; Deem, M. *Proc. R. Soc. London, Ser. A* **1991**, *433* (1889), 499.
(26) Tessier, C.; Haumesser, P.; Bernard, P.; Delmas, C. *J. Electrochem. Soc.* **1999**, *146* (6), 2059.
(27) Amatucci, G.; Tarascon, J.; Klein, L. *J. Electrochem. Soc.* **1996**, *143* (3), 1114.
(28) Miyazaki, S.; Kikkawa, S.; Koizumi, M. *Synth. Met.* **1983**, *6* (C), 211.
(29) Kikkawa, S.; Miyazaki, S.; Koizumi, M. *J. Solid State Chem.* **1986**, *62* (1), 35.
(30) Lang, G.; Bobroff, J.; Alloul, H.; Collin, G.; Blanchar, N. *Phys. Rev. B: Condens. Matter Mater. Phys.* **2008**, *78* (15), 155116.
(31) Rietveld, H. *J. Appl. Crystallogr.* **1969**, *2* (2), 65.
(32) Rouxel, J. *J. Solid State Chem.* **1976**, *17* (3), 223.
(33) Huang, Q.; Foo, M.; Lynn, J.; Zandbergen, H.; Lawes, G.; Wang, Y.; Toby, B.; Ramirez, A.; Ong, N.; Cava, R. *J. Phys.: Condens. Matter* **2004**, *16* (32), 5803.
(34) Igarashi, D.; Miyazaki, Y.; Kajitani, T.; Yubuta, K. *Phys. Rev. B: Condens. Matter Mater. Phys.* **2008**, *78* (18), 184112.
(35) Platova, T.; Mukhamedshin, I.; Dooglav, A.; Alloul, H. *JETP Lett.* **2010**, *91* (8), 421.
(36) Carlier, D.; Saadoune, I.; Croguennec, L.; Ménétrier, M.; Suard, E.; Delmas, C. *Solid State Ionics* **2001**, *144* (3−4), 263.
(37) Shaklette, L. T.; Jow, T. L. *J. Electrochem. Soc.* **1988**, *135*, 2669.